Electronic Supplementary Material (ESI) for ChemComm.

SUPPORTING INFORMATION

Liquid-to-Gel Transition for Visual and Tactile Detection of Bioanalytes

Tatiana A. Fedotova[†], Dmitry M. Kolpashchikov[†⊥*]

[†]Chemistry Department, University of Central Florida, Orlando, FL 32816, USA.

[⊥]Burnett School of Biomedical Sciences, University of Central Florida, Orlando, 32816, Florida, USA

E-mail: dmitry.kolpashchikov@ucf.edu.com

Table of Contents

1. Materials and Methods

Materials and instrumentation. DNAse/RNAse-free water was purchased from Fisher Scientific, Inc. (Pittsburgh, PA) and used for all buffers and for the stock solutions of oligonucleotides. All other oligonucleotides (see Table S1 for sequences) were obtained from Integrated DNA Technologies, Inc. (Coralville, IA). The oligonucleotides were dissolved in water and stored at -20 °C until needed. Stock concentrations of oligonucleotides were calculated by measuring the absorption of the solutions at 260 nm by using a Perkin–Elmer Lambda 35 UV/Vis spectrometer (San Jose, CA). Extinction coefficients of oligonucleotides were calculated by using OligoAnalyzer 3.1 software (Integrated DNA Technologies, Inc.)

2. Assay optimization and Experimental Procedures

2.1. Assay optimization. Our first task was to determine if acetylacetone is a substrate for peroxidase-like DNAzyme. The initial experiments were performed with full version of the aptamer sequence. We used literature- reported concentrations for peroxidase-like DNAzyme assays, which were 1 μM and 250 nM for DNA and hemin respectively[6]. Under this conditions however no polymerization was observed. Based on the fact that minimum concentration of HRP needed to catalyze polymerization of the acrylamide under the same conditions was 1 μM (data not shown), we hypothesized that peroxidase-like DNAzyme, which is inevitably less catalytically efficient than HRP, doesn't produce enough acetylacetone radicals to initiate polymerization. Also taking into account denaturing effect of the reaction buffer, which contained 40% acrylamide: bisacrylamide on the formation of G-quadruplexes as well as denaturing effects of H_2O_2 on hemin, the real concentration of the hemin-aptamer complex can be predicted to be lower than expected.

On the other hand, polymerization reaction is strongly inhibited by oxygen. This could be remedied by addition of higher concentrations of acetylacetone, as determined by Zhi-Qi Cai et al[13]. However too high concentrations of acetylacetone will lead to formation of acetylacetone polymers and not the polymerization of acrylamide. It was finally determined that peroxidase-like DNAzyme can catalyze polymerization of acrylamide into polyacrylamide, however under high concentrations of hemin and DNA (5 μM and 10 μM respectively).

2.2. Analyte-dependent polymerization assay. All experiments were carried out in the buffer, containing 50 mM HEPES, 50 mM $MgCl_2$, 20 mM K^+, 120 mM NaCl, 1 % DMSO v/v, 0.03 % w/v Triton X 100, 38 % w/v acrylamide, 2% w/v bisacrylamide, pH 6.6. Prior to polymerization experiments acetylacetone and hemin were added to the buffer solution to the final concentrations of 0.127 M and 5 μM respectively. Solution was stirred and degassed under vacuum for 30 min, after which it was distributed into the test tubes. In experiments with AMEL X and AMEL Y analytes full DNA sequence, two sensor strands and two sensor strands with analyte were added to their respective tubes to the final concentration of 10 μM each. In the experiments with ATP detection 5 mM or 10 mM ATP were added in place of DNA analytes. Following the addition of DNA strands H_2O_2 was added to each tube to the final concentration of 5.2 mM. Samples were allowed to incubate for 1 hour, after which polymerization was assessed.

3. Table S1. Oligonucleotides used in the study

Name	Sequence 5‘ ✂ 3‘	Purification[g]
PxD	GGG TAG GGC GGG TT GGG[b]	SD[c]
AMEL_Y	CTG CCT GAC CAT T CG GAT TGA CTC TTT CCT CCT AAA TA	SD
PxD4	GCA CCCC / iSp9/ GGG TA GGG[a]	SD
PxD3	GGG TT GGG / iSp9/ CC GAC TCA CAC C	SD
AMEL_X	GGC TGC AGG GTG TGA GTC GG GGGG TGC TGT TGG GAC AGC	SD
AMEL_Xmut	GGC TGC AGG GTG TGA GTC GG GGGA CGC TGT TGG GAC AGC	
PxD1	GGG TT GGG /iSp9/ ACC TGG GGG AGT A	SD
PxD2	cccT GCG GAG GAA GGT/iSp9/ GGG TA GGG	SD
PxD5	GGGTTGGG /iSp9/GCGC CGA ATG GTC AGG CAG GCGC CAG GAC ACGAG	SD
PxD6	CTCG TGT CCT G /iSp9/GGGTGGG	SD

[a]iSp9, internal triethylene glycol spacer (IDT)
[b]undelined sequence are part of PxD G quadruplex
[c]SD, standard desalting

4. Figure S1. Secondary structure of PxD_β_ATP strand.

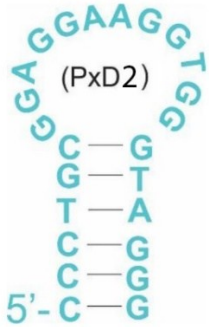

Figure S1. Secondary structure of **PxD2** strand. The structure was predicted using Mfold (M. Zuker, *Nucleic Acids Res*. 2003, **31**, 3406-3415)

Figure S2. Characterization of the gel fragments by microscopy

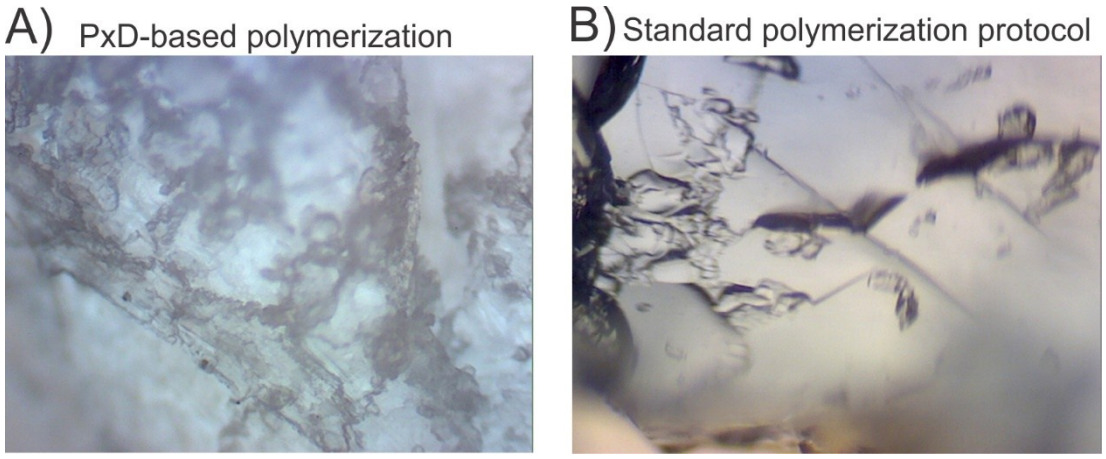

Figure S2. The gel fragments polymerized using PxD assay developed in this study as well as standard polymerization protocol (Laemmli UK Nature. 227, 680–685) (B) were viewed using microscope AmScope B120C-E1 with 40× magnification lens.

Comparison of the gel polymerized by PxD with that polymerized by the standard polymerization method (Laemmli UK Nature. 227, 680–685) under microscope did not reveal significant difference of the gel texture and hardness.